



Physical model study on the clay–sand interface without and with geotextile separator

Wei-Qiang Feng¹ · Chao Li² · Jian-Hua Yin¹ · Jian Chen² · Kai Liu¹

Received: 6 March 2018 / Accepted: 14 January 2019 / Published online: 2 February 2019
© Springer-Verlag GmbH Germany, part of Springer Nature 2019

Abstract

In most marine reclamation projects, sand fill is placed directly on soft marine seabed soils. The sand particles can easily penetrate into the soft marine soils, and the soft soil can also move into the pore spaces inside the sand at the initial contact interface between the sand and the soft marine soil. In this case, the permeability and the volume of the sand above the initial surface are reduced. To avoid this problem, a geotextile separator is often placed on the surface of the soft marine soils before placing the sand. In this study, a two-dimensional physical model is utilized to study the geotextile separator effects. The initial conditions of a clayey soil, sand fill, and surcharge loading were kept the same in the physical model test with the only difference being that a geotextile separator was either placed on the clay surface or omitted. The settlements of the initial interface were recorded and compared for the two cases without or with the geotextile separator. The particle size distribution of the soils taken across the interface zone for different time durations was then measured, analyzed, and compared. Based on an analysis of the results, the sand percolation depth was 40 mm and fine particle suffusion was apparent when the sand was placed directly on the marine slurry surface without a geotextile separator. However, when a geotextile separator was used sand percolation was avoided, and the fine particle suffusion was effectively diminished. A relative fine particle fraction is defined to illustrate the migration of fine particles from the clay to the sand soils. The fine particle percentages of the Hong Kong Marine Deposits–sand mixtures were calculated for the cases with and without a geotextile separator using an empirical formula and micromechanical modeling to obtain a better understanding of the effects of geotextile separators in practice.

Keywords Geotextile · Interface · Percolation · Physical model · Suffusion

1 Introduction

Many reclamation projects have been conducted in Hong Kong, Singapore, Australia, Malaysia, USA, etc. [18]. For new marine reclamation projects in Hong Kong, soft marine seabed soils are not allowed to be dredged and dumped at another marine site due to environmental concerns [15, 16]. In Hong Kong, sand fill is normally placed on top of the marine seabed soils using a large barge with bottom openings [10, 37]. When the sand fill reaches a level of 6–7 m above the seabed, vertical drains are installed through the sand fill into the soft marine soils with a surcharge applied by additional fill. In this way, the soft marine soils are kept in place, with a reduction in the post-construction settlements and an increase in the shear strength. However, when the sand fill is placed directly on the soft marine soils, sand percolation may occur. Sand

✉ Jian-Hua Yin
cejhyin@polyu.edu.hk

Wei-Qiang Feng
wqfeng@polyu.edu.hk

Chao Li
chao.li@chechk.com

Jian Chen
jchen@chec.bj.cn

Kai Liu
kevin-kai.liu@connect.polyu.hk

¹ Department of Civil and Environmental Engineering, The Hong Kong Polytechnic University, Hung Hom, Kowloon, Hong Kong, China

² China Harbour Engineering Company Limited, North Point, Hong Kong, China

percolation is the process by which the sand particles migrate into the clayey soils along the depth. Based on engineering experience, some sand particles percolate into the soft marine slurry at the interface between the sand fill and the marine slurry; this can result in the loss of sand above the initial contact interface and into the marine soils near the interface, which then becomes a clay–sand mixture [31]. It is therefore necessary to consider sand percolation in the design of any reclamation project.

For clay–sand mixtures, much research has focused on the experimental study on the influence of sand content on the shear strength [23, 35, 38] and consolidation properties [17, 32, 38]. Monkul and Ozden [25] conducted oedometer tests on the compression characteristics of kaolinite–sand mixtures. Peters and Berney [27] investigated the influence of fine fraction on the threshold behavior and stable force chains of clay–sand mixtures. Simpson and Evans [34] examined the behavioral thresholds of clay–sand mixtures with fine contents ranging from 0 to 100%. Choo et al. [9] studied the compressibility and small strain stiffness of kaolinite–sand soils consisting of a high clay particle content and proposed a porosity function of small particles. Park and Santamarina [26] summarized the basic properties and mechanical behavior of coarse–fine mixtures from previous studies and proposed a revised soil classification system to capture the mechanical and hydraulic properties. Shi and Herle [29, 30] proposed a general procedure for the mechanical evaluation of inhomogeneous soils with stiff inclusions. This approach was further generalized by Shi and Yin [32] for the consolidation behavior of marine–sand mixtures based on a series of oedometer tests. The model has only three parameters with clear physical significance, which may have potential application in practice. Most of the researches on clay–sand mixtures have used element tests, including oedometric and triaxial compression tests, and the clay–sand mixtures are manually prepared. These tests have provided the experimental evidence of the clay particle content for investigating the fundamental behavior of soil mixtures. However, there has been little experimental modeling conducted to directly study the amount of percolation at the clay–sand interface.

Fine particle suffusion, as one type of internal erosion, is used to describe the fine soil particle transport through the pore domain in a coarse layer by seepage flow [3]. Fine particle transport can induce internal instability such as piping and sinkholes [14, 20], and a significant amount of clayey soils can be lost in the process of suffusion. It is difficult to quantitatively evaluate the amount of clayey soils lost to suffusion and the consequent instability of the marine clay layer in reclamation projects. However, the fine particle amount is usually measured in the laboratory tests [22, 36]. Based on the mass balance equation, the fine particle suffusion can result in a change in the particle size

distribution (PSD) of the original soils. As a result, a comparison of PSDs of soils measured before and after fine particle movement is an effective means for evaluating the amount of fine particle transport and fine particle suffusion.

It has been suggested that a geotextile sheet be used as a separator and placed on the marine soil surface before adding the sand fill, with the aim of minimizing the sand percolation effects in marine reclamation projects in Hong Kong. The geotextile separator also plays a significant role in minimizing the generation of mud waves, by confining the sub-sea marine mud and stabilizing the filled area. This approach has been used in several projects including the Pak Shek Kong reclamation in Hong Kong [24], the Changi east reclamation in Singapore, the New Kita-Kyushu airport in Japan etc. [10]. However, it is still unclear how efficient geotextile separators are at the clay–sand interface. In Hong Kong, marine reclamation for the construction of the airport third runway system is about to start. Clean sand will be placed on the surface of Hong Kong Marine Deposits (HKMD) under seawater. However, whether or not a geotextile separator shall be placed on the surface of HKMD has yet to be decided; the effects and efficiency of geotextile separators need to be fully understood. This is main motivation of our research project.

In the field, the actual marine and geotechnical conditions are usually very complicated. A physical model that represents the typical field conditions with initial controllable conditions will be used. The HKMD and sand used in the physical model were taken from an existing marine reclamation project in Hong Kong. This physical model with the same HKMD was divided into two parts: one part did not have a geotextile separator, while the other part used a geotextile separator between the HKMD and sand fill. The same sand was placed on the surface of the HKMD slurry in the model, and the same multi-stepped vertical loading was applied. The main goal of the physical model is to study the sand percolation and fine particle suffusion that occurs during the sand filling and consolidation process of the HKMD when the geotextile separator is not utilized. This is very beneficial for engineers to determine the fine particle travel boundary. By comparing the results of sand–clay interface without and with a geotextile separator, the effects of the geotextile separator in reclamation projects can be investigated and assessed.

2 Physical model and experimental procedures

2.1 Physical model and materials

A plane strain physical model, designed by Yin and Fang [39], was adopted in this study. This model has the

dimensions of 900 mm (in length), 300 mm (in width), and 900 mm (in depth). This physical model has two transparent sides of 25.4 mm thickness with adhered rulers and marked horizontal lines (as shown in Fig. 1), which were used to monitor the real-time settlement of the HKMD–sand interface. In order to investigate the effects of a geotextile separator, one-third (300 mm) of the length (900 mm) of the physical model space had a geotextile separator placed directly on the HKMD slurry.

The HKMD was taken from the East Coast of Lantau Island in Hong Kong. The initial water content of the HKMD was 44–52%. This HKMD was mixed with water using a miniature motorized mixer [39]. The prepared water content of the HKMD slurry was controlled in the range of 105–110%, which was around 2 times of the liquid limit of the HKMD. The clean sand, used in the field as the sand fill, was chosen for this physical model study. A special sand layer dyed orange was placed on the HKMD surface adjacent to the transparent sides. The geotextile separator used in the physical model test was of the same type to be used at the site. The basic properties of the geotextile separator are listed in Table 1. The initial PSD curves of the sand fill and the HKMD are shown in Fig. 2.

2.2 Description of test procedures

Detailed test procedures are as follows:

Firstly, the HKMD marine clay slurry, with an initial water content of 105–110%, was poured into the model apparatus that has a length of 900 mm. The initial height of the slurry in both the left and right sides was 750 mm. After one night's initial consolidation of the marine clay slurry under its self-weight, there was approximately a 5-

mm settlement at the clay surface and some clean water was observed. The initial undrained shear strength C_u of the marine slurry was measured using a mini shear vane and varied between 0.1 and 0.2 kPa due to the high initial water content. Secondly, the sand layers were uniformly sprayed onto the marine clay surface for both sides of the test apparatus. A container with a length of 630 mm and width of 300 mm was used to spray the sand uniformly on the surface of marine slurry. The sand was uniformly sprayed to a 10 mm thickness at 30-mm marked intervals, as shown in Fig. 3. The sand layer with a marked length of 30 mm was carefully scraped off from the container to the soft marine soil. This procedure was done stepwise until the marine slurry surface was completely covered by sand. It was observed that the first 20 mm of the sand fill was nearly infiltrated into the marine clay when there was no geotextile separator at the HKMD–sand interface. Once the sand fill reached 70 mm, it was left for 1 h to record the interface location. Sand fill was then added to 150 mm and kept for 1 h to record the interface location.

In order to apply the vertical loading uniformly, a rigid plate of 30 mm × 30 mm with evenly distributed holes was placed on the filled sand surface, and a 5 kPa vertical pressure was applied by a dead weight for 1 h. The pressure was then increased to 10 kPa and left for 12 h. Settlement values at 1 h, 4 h, and 12 h were recorded. After this, the pressure was increased to 15 kPa using dead weights and kept for 12 h. Settlements at 1 h and 12 h were recorded. Finally, the vertical pressure was increased to 20 kPa and left for 819 h. The wet towel was put on the surface of the rigid plate to prevent the evaporation of pore fluids during this time. Figure 4 shows the process of preparing the physical model and adding vertical stresses. The relationship of applied vertical stress versus time is presented in Fig. 5.

2.3 Shear vane tests

After 10 days of preloading, the dead weights applying 20 kPa of vertical stress were removed and the first shear vane test was conducted to investigate the undrained shear strength of the soils. Afterward, the vertical stress was reloaded to 20 kPa. A second shear vane test was conducted after 10 days of reloading. The dead weights were reapplied after the second shear vane test and a third shear vane test were conducted after a further 10 days. Figure 6 shows the locations of the first, second, and third shear vane tests, in which the side friction effect and soil disturbance of the shear vane tests were considered. In this study, a handy mini vane tester, 33 mm in diameter and 55 mm in height, was utilized to quickly and accurately determine the undrained shear strength of the soils. The shear vane tests were conducted at intervals of 40 mm

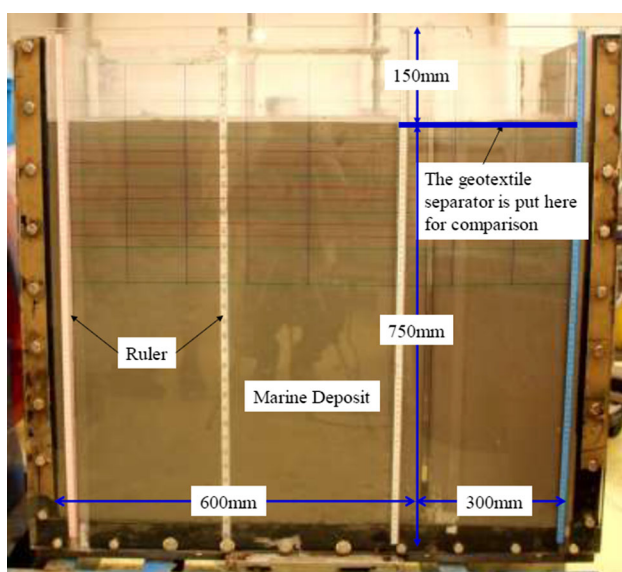


Fig. 1 Setup of the physical model

Table 1 Properties of geotextile separator used in the physical model

Pore size O_{90} (mm)	Tensile strength (kN/m)	Permeability ($l/m^2/s$)	Stable temperature ($^{\circ}C$)	Life period (year)
0.1	100	20	0–60	60

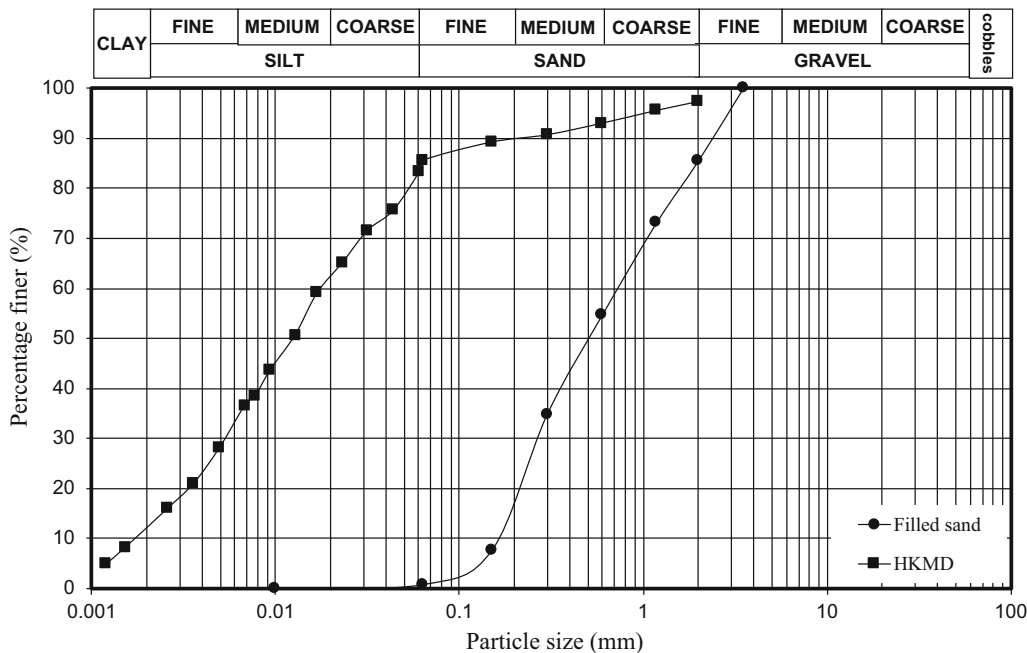


Fig. 2 Particle size distributions of HKMD and sand used in the experiment

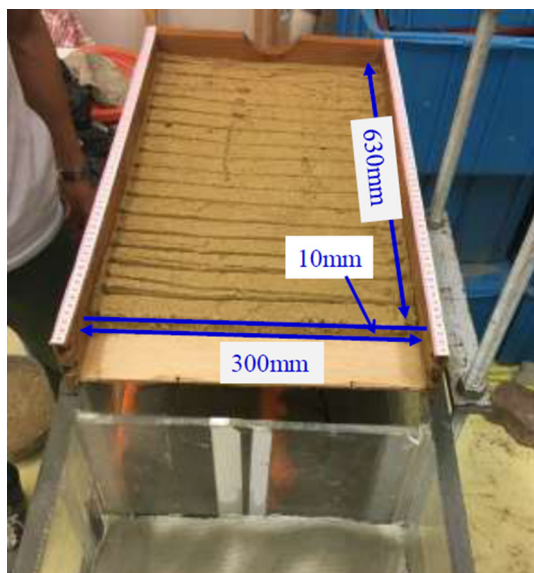


Fig. 3 Spraying the sand on the surface of the marine clay slurry

along the depth. For accuracy, each shear vane test was measured at two or three different locations at different depths, as shown in Fig. 6. For the HKMD–sand interface with the geotextile separator, the undrained shear strength

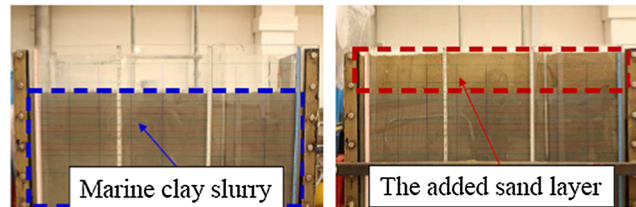
was not measured because the mini shear vane tester could not easily penetrate the geotextile separator.

2.4 Particle size distribution analysis

To directly quantify the amount of sand percolation at the interface, one approach is to analyze the PSDs of the soils across the initial interface between the sand and the HKMD slurry. The PSD of HKMD soil can change due to sand percolation in the interface zone. Similarly, the PSD of sand above the initial interface might vary due to fine particle suffusion from the HKMD below the interface zone. Fine particles are referred as the soil particles passing through a standard sieve with an opening size of 0.063 mm. Supposing that HKMD has a fine content by weight of M_{clay} and the original sand has a fine content by weight of M_{sand} , the fine content of the HKMD–sand mixture is $M_{mixture}$ at the HKMD–sand interface. A relative fine particle fraction (denoted as Θ) is the ratio of migrated fine particles of clay–sand mixtures to the fine particles of clayey soils, expressed as:

$$\Theta = \frac{M_{mixture} - M_{sand}}{M_{clay}} \tag{1}$$

(a) Preparation of the physical model



(b) Loading procedures of the physical model

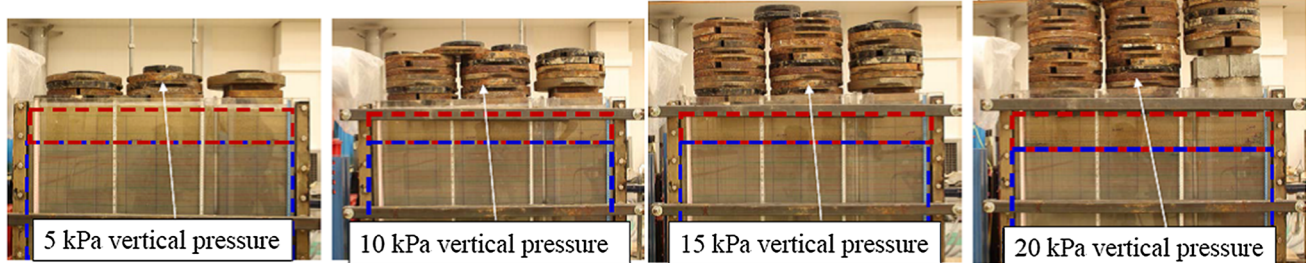


Fig. 4 Loading procedures of the physical model

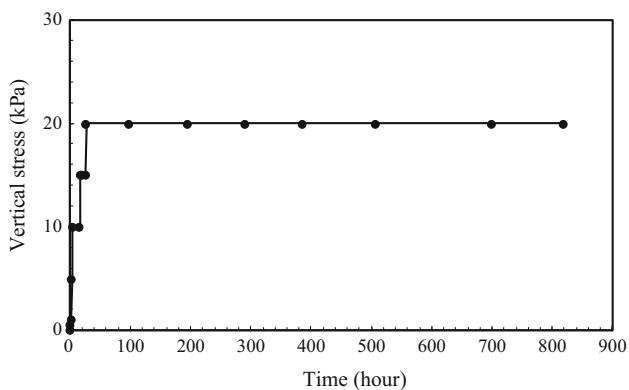


Fig. 5 Applied vertical stress on the surface of the sand with time

In this study, there are fewer fine particles in original sand fills, $M_{\text{sand}} = 0.1\%$. It is expected that the value of Θ is in the range of 0–1, which is an indicator of the migrated fine particle percentages due to sand percolation and fine particle suffusion effects.

To analyze how the PSD varied with depth through the HKMD–sand interface region, a square hole of 50 mm × 50 mm was excavated from the sandy soil surface. Soil samples at different depths were removed for particle size tests and analysis at depths of 0–40 mm, 40–80 mm, 80–100 mm, 100–120 mm, 120–140 mm, and 140–160 mm, as illustrated in Fig. 7. Details of the soils at each depth were photographed (see Fig. 7). It is worthwhile noting that the thin layer of colored sand scattered at the interface before adding the sand fill to the surface of HKMD was detected at a depth of 100–120 mm. The sandy soils taken from different depths were then sieved using the

dry sieving method (from 0.063 to 2 mm). After sieving, the samples were oven-dried for 1 day. Finally, the dry mass of the samples was measured, and the PSD was determined. The hydrometer method was used to analyze the PSD of the HKMD [7]. For the HKMD–sand interface with a geotextile separator, a similar approach was used to obtain the PSD for the sandy fill soil and the HKMD.

3 Test results and discussions

3.1 Settlement of the HKMD–sand interface

A side view of the settlement profile at different times is shown in Fig. 8a, and the curves of the average settlement versus time at the HKMD–sand interface are shown in Fig. 8b for the two cases with or without a geotextile separator. As stated above, the initial conditions (HKMD, sand, and loading) for the interface with or without the geotextile separator were the same in the physical model, which minimizes the soil heterogeneity. The settlement difference can therefore be assumed to be directly related to the effects of the geotextile separator.

It is found from Fig. 8 that the rate of interface settlement at the initial stage is relatively large due to the initially large void ratio of the soils near the HKMD–sand interface. Afterward, a decrease of the void ratio near the interface zone induces a decrease in the permeability of the sand, which reduces the drainage speed of water through the interface zone. Initially, the settlement of the HKMD–sand interface with the geotextile separator is the same as without a geotextile separator, as shown in Fig. 8. After

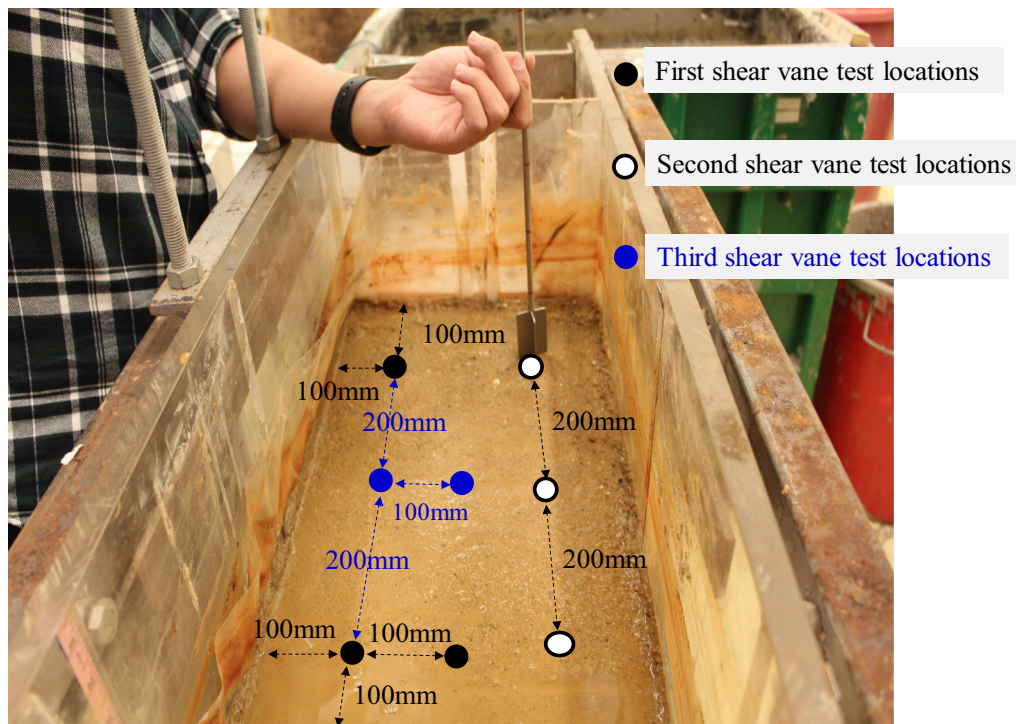


Fig. 6 Locations of mini shear vane tests

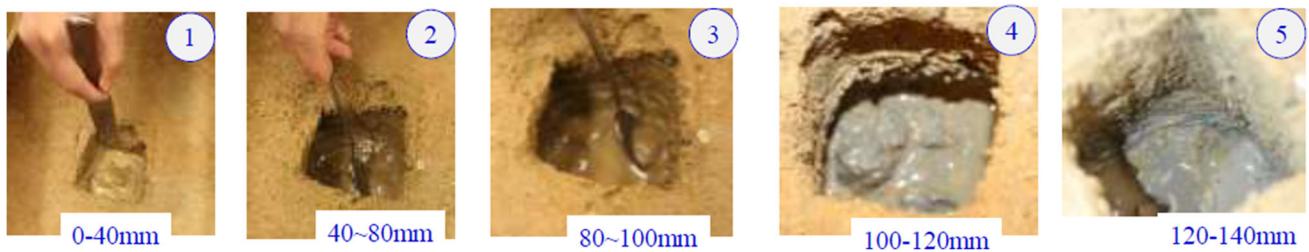


Fig. 7 Soil samples taken at different depths for particle size analysis

240 h (10 days), there is a difference in the two settlement–time curves, as shown in Fig. 8b. This indicates that the

geotextile separator gradually prevents sand percolation and fine particle suffusion at the interface zone. The

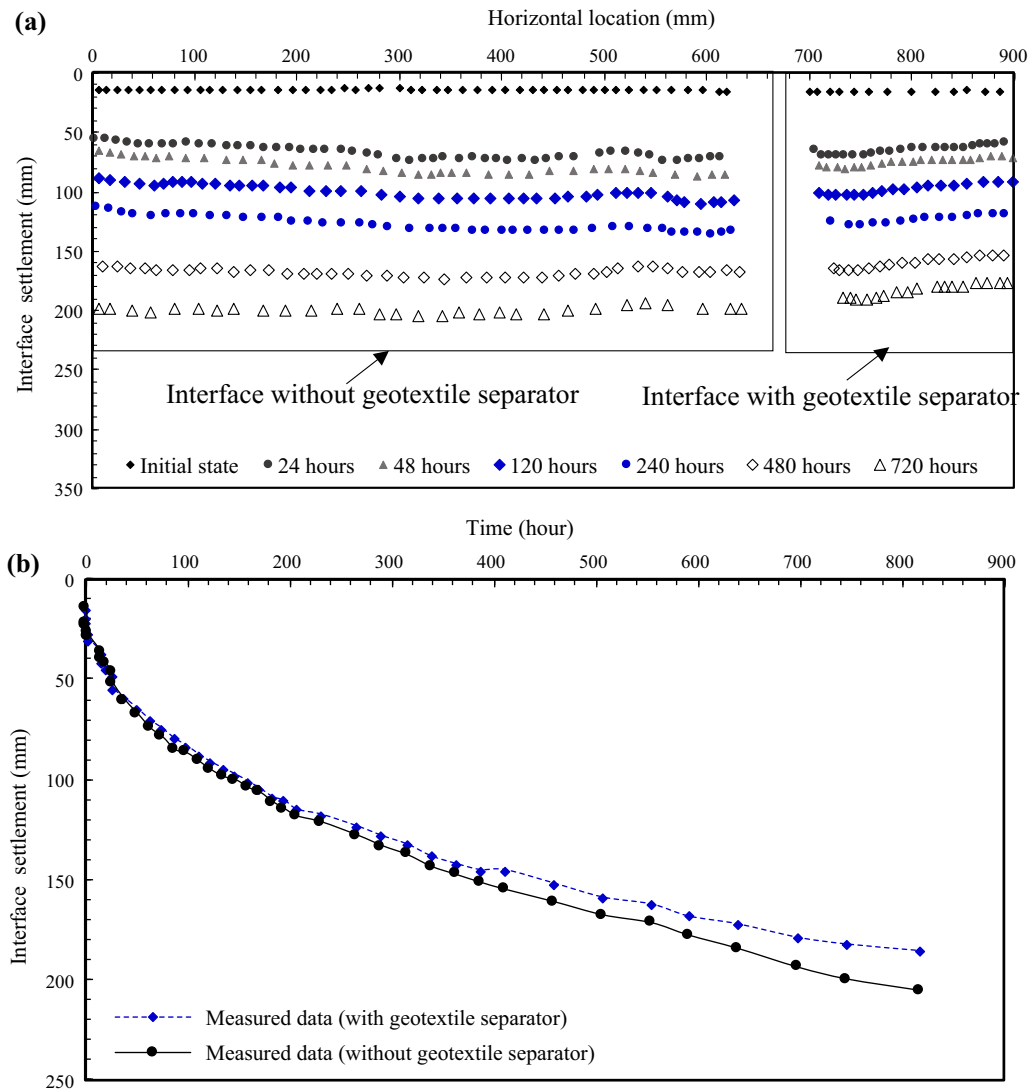


Fig. 8 Measured interface settlements with time in the physical model without or with geotextile separator: **a** side view of the settlement profiles at different times and **b** average settlement versus time

settlement difference between the HKMD–sand interface without a geotextile separator and the one with the geotextile separator increases up to 25 mm by the end of the test, as shown in Fig. 8. It should be noted that this settlement difference was caused by the geotextile separator mainly in the consolidation stage of the HKMD. In actual marine reclamation projects, the sand placement method, the relative density and shape of the sand particles, and site environment factors such as tides, waves, and the marine soil conditions (heterogeneity, shear strength, permeability, etc.) may contribute to mud waves and settlements of the reclamation.

3.2 Results of the shear vane test

The shear vane test is a relatively practical and inexpensive test, which is accurate and effective for measuring the undrained shear strength of clayey soils. The undrained shear strength is closely related to the fine particle content in the interface transition zone [25]. The undrained shear strength of the soils with the depth through the HKMD–sand interface region without a geotextile separator was measured using a mini vane tester at 10, 20, and 30 days after the first loading. The measured undrained shear strength along the depth at 10, 20, and 30 days is shown in Fig. 9.

For the first shear vane test, the top surface of the mini shear vane was 20 mm beneath the surface of the HKMD. The effective middle depth of the vane corresponding to

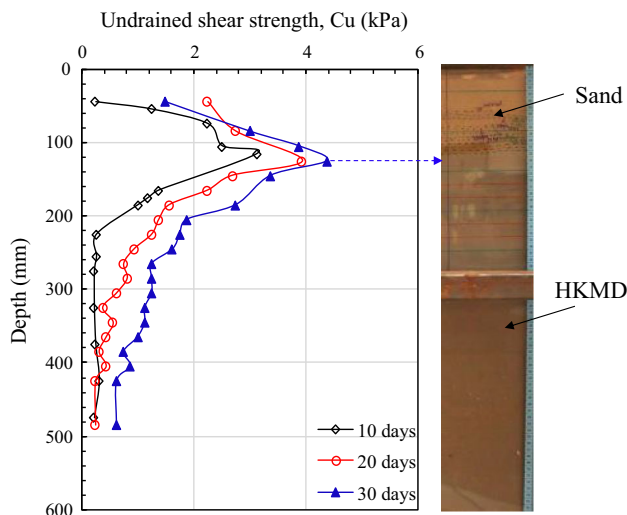


Fig. 9 Measured undrained shear strength values with depth through HKMD–sand interface without a geotextile separator at 10, 20, and 30 days

the measured undrained shear strength was 45 mm. It can be seen from Fig. 9 that the undrained shear strength (USS) values at durations of 10, 20, and 30 days were low near the sand fill surface, but increased with depth, reaching maximum (peak) values at locations in the vicinity of the sand–HKMD interface. After the peak values, the USS values decreased with depth. The maximum values of the undrained shear strength were 3.2 kPa, 3.9 kPa, and 4.4 kPa for durations of 10, 20, and 30 days, respectively, as shown in Fig. 9. Due to consolidation, the USS increases with time. Considering the relatively large permeability of the sand and the 100 mm thickness of the sand layer, the sand above the HKMD–sand interface was close to a drained condition. Therefore, the increase in the USS at the HKMD–sand interface zone resulted from a variation in the sand content.

3.3 Observation of the excavated hole and PSD analysis

As mentioned above, a square hole was excavated in the center of the physical model, and soil samples were taken at different depths after 10 days, 20 days, and 30 days, respectively, for PSD tests and analysis. Figure 10 shows the location of the initial interface between the HKMD and the sandy soil fill because of the orange-colored sand particles. The sand above the interface has become a greyish color, which indicates that the HKMD clayey soil particles have moved into the sand layer above. Figure 10 also shows evidence of sand percolation below the HKMD–sand interface. The orange color sand was initially between the sand fill and the HKMD surface. When we removed HKMD from below the interface, sand particles

could be felt, indicating sand percolation. Therefore, a transition zone was formed near the initial HKMD–sand interface, where sand percolated into the HKMD clayey soil and fine clay particles suffused into the sand layer above.

To quantitatively estimate the percolation depth, soil samples were taken from different depths in the physical model for PSD tests. Note that the coordinate for the sand surface was denoted as 0. The ones below this surface are assumed to be positive. Figure 11 presents a comparison of the PSD for the soils and the fine particle percentages at different depths across the HKMD–sand interface zone without a geotextile separator after 30 days of 20 kPa pressure. The fine particle percentage of the original sand fill was 0.1%, and the fine particle percentage of the original HKMD was 84.7%. After 30 days, the PSD curve at the top 40 mm is close to the original sand material, and the fine particles increase slightly with the depth until the clay–sand interface zone (80–100 mm). The fine particle percentages of the sandy soil varied from 0.8 to 1.8% when there was no geotextile separator, as shown in Fig. 11b. This is because some fine particles of HKMD can be transported into the sand layer during the consolidation stage, as illustrated in the fine particle suffusion diagram of Fig. 11b. At a depth of 100–120 mm, the PSD curve changes significantly, and the fine particle percentage is 42.2%, indicating the percolation effects at the clay–sand interface. Below that, the PSD curve at 120–140 mm is slightly different from that of 140–160 mm, which has also been affected by sand percolation, i.e., some fine particles of sand fill the inter-particle voids. The PSD curve at a depth of 140–160 mm is the same as that for the original HKMD. Therefore, in this study, the thickness of sand percolation is 40 mm.

Similarly, the PSD curves of the soils recovered from different depths and the fine particle percentages across the clay–sand interface when a geotextile separator was installed are shown in Fig. 12. It is found that the PSD curve at 0–40 mm almost overlaps that from 40 to 80 mm, as shown in Fig. 12a. The fine particle percentages of soils above the interface are in the range of 0.22–0.55% for the HKMD–sand interface with a geotextile separator (Fig. 12b). There is a slight difference in the PSD from depths of 80–100 mm and 100–110 mm. This difference is a result of fine particle suffusion. Below the geotextile at 110–120 mm, the PSD of the HKMD is the same as the original HKMD, which indicates that the geotextile separator prevents sand particles percolating into the clayey soils.

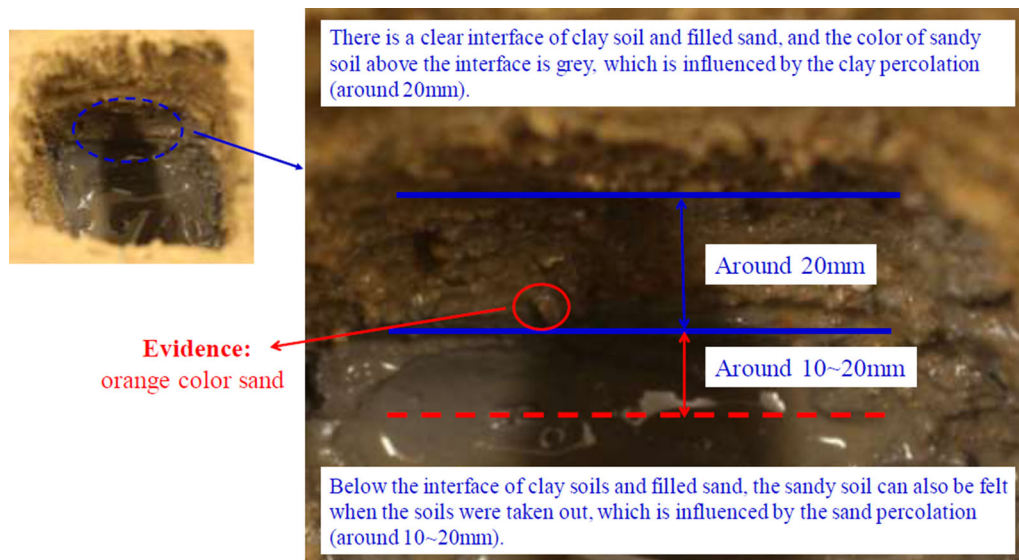


Fig. 10 Observation of the movement of HKMD slurry above and sand below the HKMD–sand interface without a geotextile separator

3.4 Analysis and discussion of the effects of a geotextile on the clay–sand interface

Taking the relative fine particle fraction as an indicator, Fig. 13 shows the effects of using a geotextile by comparing the results from the clay–sand interface with and without a geotextile separator in this experimental model.

As shown in Fig. 13a, the original interface becomes a transition zone for the clay–sand interface when there is no geotextile separator; the sand particles percolate nonlinearly into the clayey soil along the depth. The relative fine particle fraction varies from 0.1 to 0.953 at a depth of 100–160 mm if there is no geotextile separator, while the fine particle fraction is 0.962 at a depth of 100–110 mm when a geotextile is used to separate the HKMD from the sand fill. Thus, the geotextile separator can effectively prevent sand particles from percolating into the clay surface if a proper geotextile separator is adopted. The shadow area in Fig. 13a illustrates the effect of the geotextile on sand percolation in this experiment. Above the clay–sand interface, Fig. 13b shows the relative fine particle fraction along the depth. For the sands taken from 0 to 80 mm, the relative fine particle fraction values are 0.0072–0.0089 for the clay–sand interface region without a geotextile separator, whereas when a geotextile separator is employed, the fine particle fraction is 0.0014–0.0017. For the sand taken from 80 to 100 mm, a lot of fine particles have been transported into the sand through the suffusion process and the fine particle fraction is up to 0.019 for the clay–sand interface region when no geotextile separator is used. However, with the geotextile separator and at the same depth, the fine particle fraction for the HKMD–sand

interface is 0.005. Therefore, the geotextile separator can significantly reduce the suffusion of fine particles.

Limited research has focused on fine particle migration through the clay–sand interface during the consolidation stage. Sterpi [36] proposed an empirical relationship for migrated fine particles in a sand–clay mixture, the hydraulic gradient, and time due to suffusion. In fact, the soils in the interface zone represent a double-porosity medium [5, 8, 28]. Bonelli and Marot [3] explained that soil suffusion is an interfacial process and derived a suffusion law to quantify the amount using a multi-scale approach. This has been further developed to describe the behavior of clay–sand mixtures [40, 41]. Subsequently, Golay and Bonelli [19] used a finite element numerical model to simulate the clay–water interface erosion process. However, these finite element simulations are mostly based on the homogenization of soils at the interface. In our experimental model, the fine particle migration decreases nonlinearly with the distance of the clay–sand interface due to deposition and clogging in the seepage flow regime. Furthermore, Chung [11] and Ho [21] observed a bridge network behind the geotextile separator, which helps prevent fine particles of clay moving into the sand particles. The study in this paper provides the evidence for this opinion.

3.4.1 The empirical relationship for particle migration

Sterpi [36] proposed a relationship for migrated fine particles in a sand–clay mixture M_{mixture} , with a hydraulic gradient i_w , and time t due to suffusion, expressed as

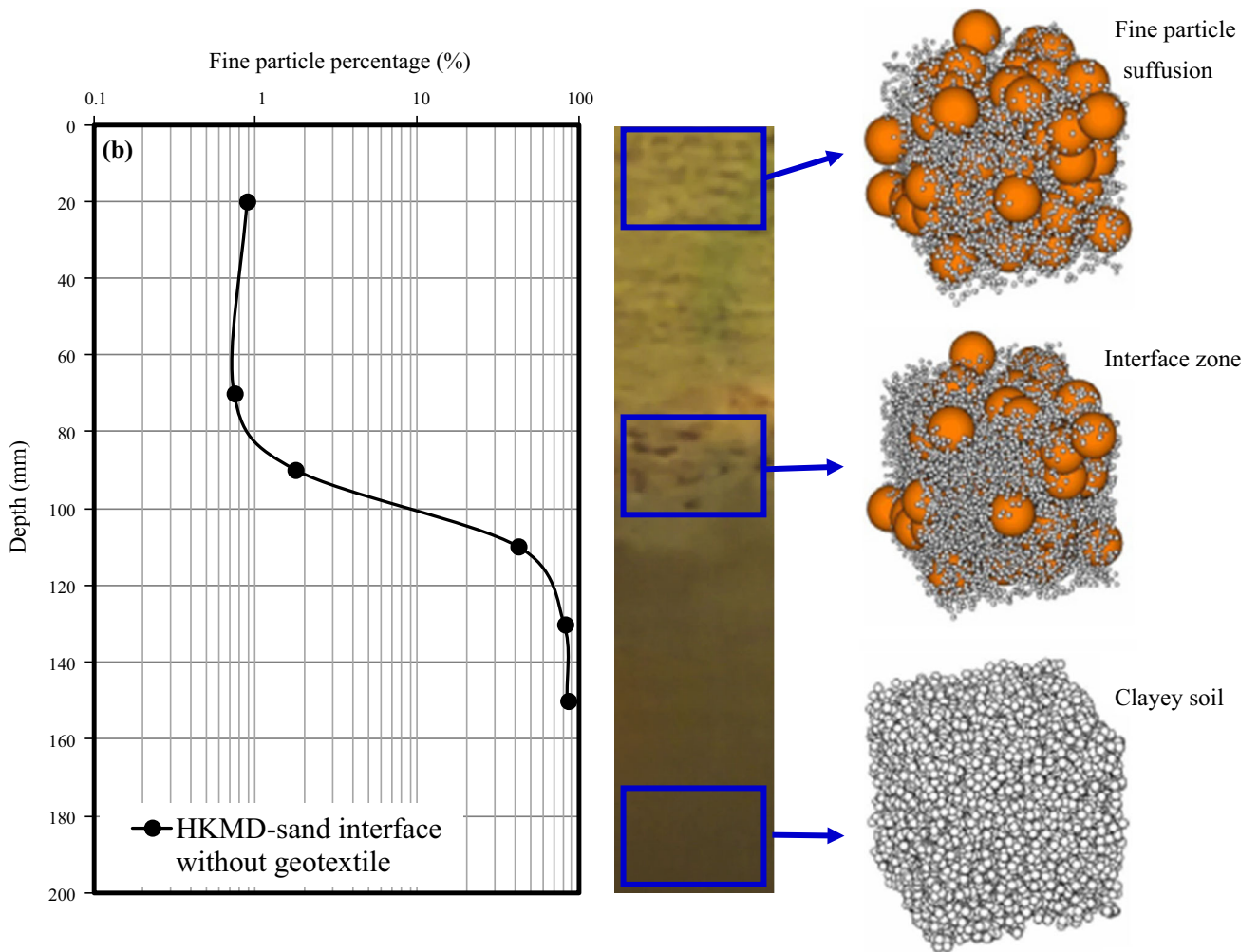
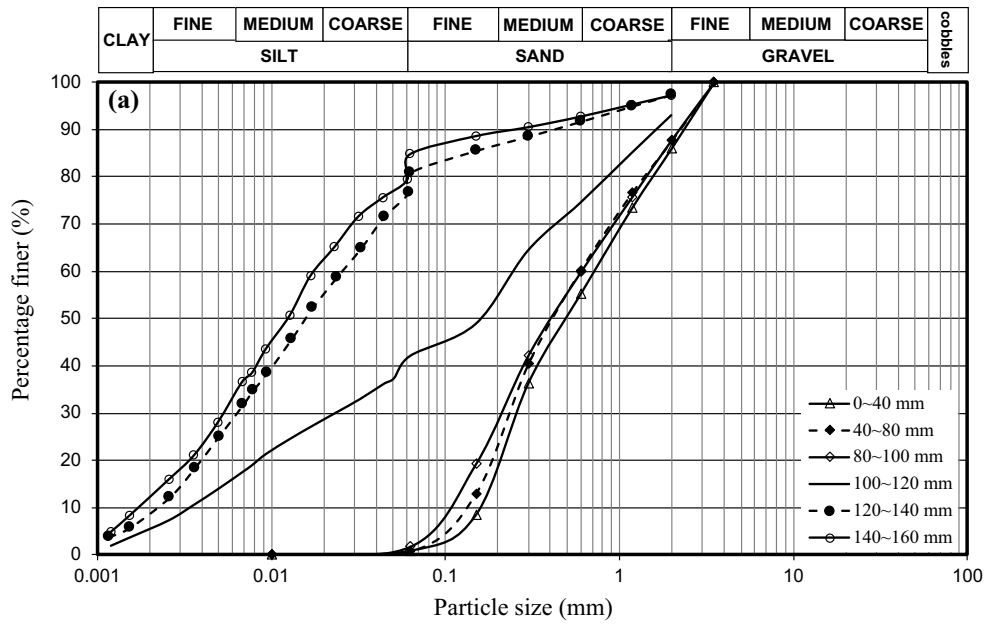


Fig. 11 a Particle size distributions of the soils taken at different depths across the HKMD–sand interface without geotextile separator and **b** fine particle percentage distributions along depth for the interface without geotextile separator

$$\Theta = 1 - \exp \left\{ - \left(\frac{i_w^c}{a} \right) \left(\frac{t}{t_o} \right)^b \right\} \quad (2)$$

where $t_o = 1$ h; t is the consolidation time; a , b , and c are three fitting parameters; i_w is the hydraulic gradient, which is related to the hydraulic load and the distance of the flow path

$$i_w = \frac{1}{\gamma_w} \frac{\partial \sigma_z}{\partial x} \quad (3)$$

where σ_z is the applied stress, i.e., $\sigma_z = 20$ kPa; γ_w is the water specific weight ($\gamma_w = 10$ kN/m³); x is the suffusion depth. In this study, the consolidation time at a pressure of 20 kPa was 819 h. The hydraulic gradient of sand is a constant since flow of most soils can be considered as laminar. The hydraulic gradient is related to the hydraulic load and the distance of the flow path. Because the surcharge loading was 20 kPa, the hydraulic gradient is assumed to be linear to the suffusion depth ($x = 0.1$ m). Thus, $i_w = 20$. Substituting Eq. (2) into Eq. (1), we obtain

$$M_{\text{mixture}} = M_{\text{clay}} \left[1 - \exp \left\{ - \left(\frac{i_w^c}{a} \right) \left(\frac{t}{t_o} \right)^b \right\} \right] + M_{\text{sand}} \quad (4)$$

Values of the fine particle fraction, Θ , in Fig. 13b are utilized to determine the exact values of a , b , and c . The least squares method in the back-calculation was used in order to minimize the discrepancy between the calculated results, Θ_{cal} , and the experimental results, $\Theta(i_w, t)$, due to the fine particle suffusion [36]

$$E(a, b, c) = \sum_{\min} [\Theta_{\text{cal}} - \Theta(i_w, t)]^2 \quad (5)$$

The best fitted parameters, with $a = 1200$, $b = 0.23$, and $c = 0.4535$, were utilized for clay–sand mixtures above the clay–sand interface without a geotextile separator. As a comparison, the values of $b = 0.23$ and $c = 0.4535$, which are related to time and hydraulic gradient, should be kept the same, and $a = 5000$ was utilized in the least squares to consider the effect of the geotextile separator on the clay–sand mixture. By using Eq. (4), the fine particle percentages of the clay–sand mixture at a depth of 100 mm, which is close to the clay–sand interface, can be predicted with the consolidation time, as shown in Fig. 14.

3.4.2 The micromechanical modeling of particle migration in interfacial erosion

As described above, the soils in the sand–clay interface zone are typical multiphase materials exhibiting two dominant porosity values, making it a double-porosity medium [5, 8]. To consider the particle migration at the clay–sand interface, the basic concepts of mass and pore scales in double-porosity media are adopted and the interfacial erosion law in the micromechanical scale is required.

As suggested in the poromechanical framework for double-porosity media [6, 8], the porous medium can be divided into the solid matrix with micropores and macropores with a representative elementary volume (REV), as illustrated in Fig. 15. The soil structure and pores are according to Zeevaart [42]. When the soils at the sand–clay interface region are saturated, the mass density and volume fractions of the mixture are expressed as

$$\phi_{\text{sand}} = \frac{\Omega_{\text{sand}}^m}{\Omega}, \quad \phi_{\text{macro}} = \frac{\Omega_{\text{macro}}}{\Omega}, \quad (6)$$

$$\psi_{\text{fine}} = \frac{\Omega_{\text{fine}}}{\Omega} \quad \text{in macroscopic scale}$$

$$\phi_{\text{micro}} = \frac{\Omega_{\text{micro}}}{\Omega_{\text{fine}}}, \quad \phi_{\text{fine}} = \frac{\Omega_{\text{fine}}^m}{\Omega_{\text{fine}}} \quad \text{in microscopic scale} \quad (7)$$

There is an important connection of the porosity domain to the macropore and the micropore densities, expressed as

$$\phi_{\text{pore}} = \phi_{\text{macro}} + \psi_{\text{fine}} \phi_{\text{micro}} \quad (8)$$

Similarly, the relationship in the solid domain between the sand particles and the fine particles is given as

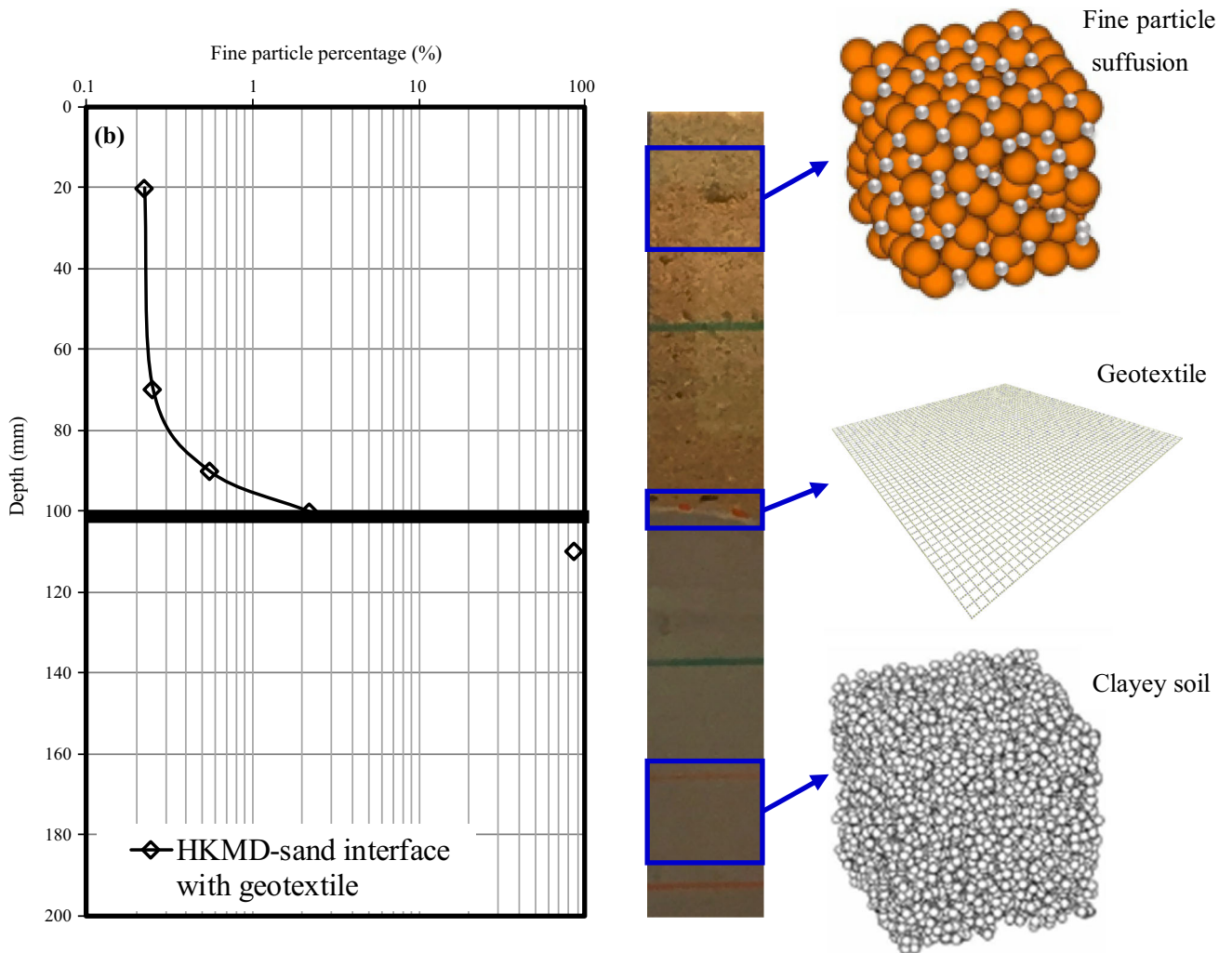
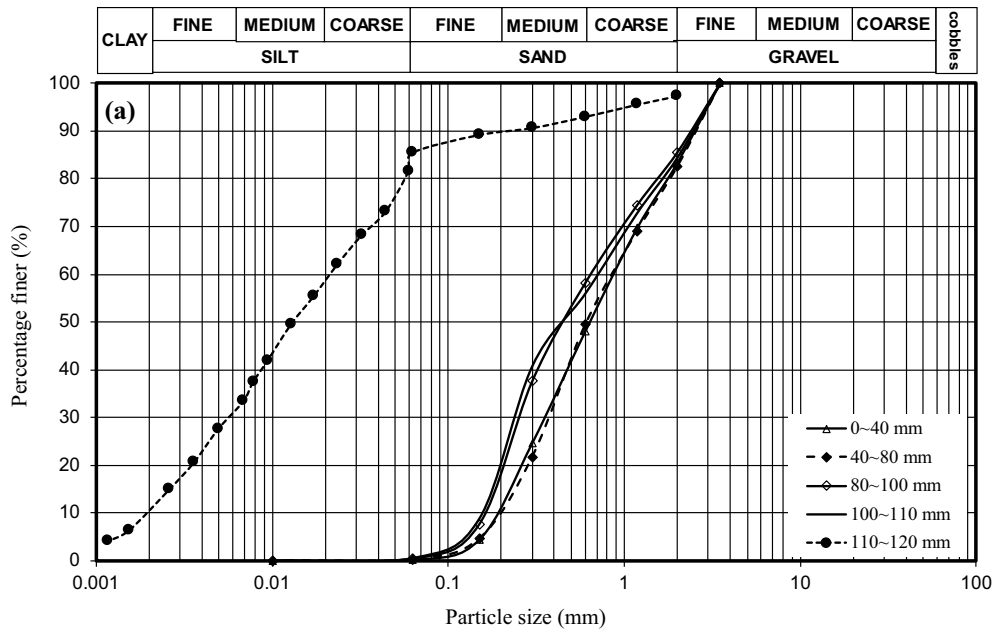
$$\phi_m = \phi_{\text{sand}} + \psi_{\text{fine}} \phi_{\text{fine}} \quad (9)$$

The fine particle migration occurs when $0 < \psi_{\text{fine}} < 1 - \phi_{\text{sand}}$. It is unreasonable to assume that all the fine particles in the REV can transfer to the sandy soils, which is the assumption in previous studies for pipe flow with erosion [2, 4], because the particle migration is also related to the density and particle uniformity of the filled sands or the pore size of the geotextile separator. Therefore, we introduce a reduction factor to account for the clay–sand interface

$$\psi_{\text{fine},s} = \delta \psi_{\text{fine}} \quad (10)$$

where δ is the reduction factor; $\psi_{\text{fine},s}$ is the particles for the migration.

Interfacial erosion with threshold laws, which is induced by tangential shear stress, is utilized here to describe the eroded materials [2]



◀**Fig. 12 a** Particle size distributions of the soils taken at different depths in the sample with a geotextile separator at the interface and **b** fine particle percentage distributions with depth with a geotextile separator at the interface

$$m = \frac{1}{\Omega|\Gamma_{\text{pore}}|} \int \dot{m}d\Gamma = \frac{1}{\Omega|\Gamma_{\text{pore}}|} \int k_{\text{er}}H\tau - \tau_cd\Gamma \tag{11}$$

where m is the interfacial erosion material; Γ_{pore} is the porosity boundary; \dot{m} is the interfacial erosion rate; k_{er} is the coefficient of surface erosion; $H[\tau - \tau_c]$ is the Heaviside step function; τ is the tangential shear stress; τ_c is the threshold stress. Other researchers have also proposed similar relationships to study particle migration using the finite element method [1, 12, 13, 33].

Bonelli and Marot [4] proposed a spatial averaging method to approximate the suffusion law

$$m = \gamma_w k_{\text{er}} \phi_{\text{macro}} \varsigma \frac{|\Gamma_{\text{er}}|}{|\Gamma_{\text{pore}}|} i_w \tag{12}$$

where ς is the quantity that accounts for the relationship between the local permeability gradient and the global pressure gradient; for the sake of simplicity, this is taken as 1 (assuming low tortuosity and weak inhomogeneities

during the consolidation stage). The surface fraction Γ_{er} of suffusion material has the following relationship with Γ_{pore}

$$\frac{|\Gamma_{\text{er}}|}{|\Gamma_{\text{pore}}|} = \frac{1}{2} H \left[\psi_{\text{fine},s} - \psi_{\text{fine},s}^{\text{stop}} \right] \left(\frac{\psi_{\text{fine},s}}{1 - \phi_{\text{sand}}} \right)^{2/3} \times \left\{ 1 - \left(\frac{\psi_{\text{fine},s}^{\text{stop}}}{\psi_{\text{fine},s}} \right)^{2/3} \right\} \tag{13}$$

$$\psi_{\text{fine}}^{\text{stop}} = \psi_{\text{fine},s}^0 \left(\frac{i_c^0}{i_c^0 + i_w} \right)^{3/2} \tag{14}$$

Following the principle of solid mass balance, we obtain

$$\frac{\partial \psi_{\text{fine},s}}{\partial t} = \frac{m}{\rho_{\text{clay}}} \tag{15}$$

Substituting Eqs. (11), (12), and (13) into Eq. (14), the following equation is obtained

$$\frac{\partial \psi_{\text{fine},s}}{\partial t} = \frac{\gamma_w k_{\text{er}} \phi_{\text{macro}} \varsigma i_w}{2\rho_{\text{clay}}} \left(\frac{\psi_{\text{fine},s}}{1 - \phi_{\text{sand}}} \right)^{2/3} \times \left\{ 1 - \left(\frac{\psi_{\text{fine},s}^0}{\psi_{\text{fine},s}} \right)^{2/3} \left(\frac{i_c^0}{i_c^0 + i_w} \right) \right\} \tag{16}$$

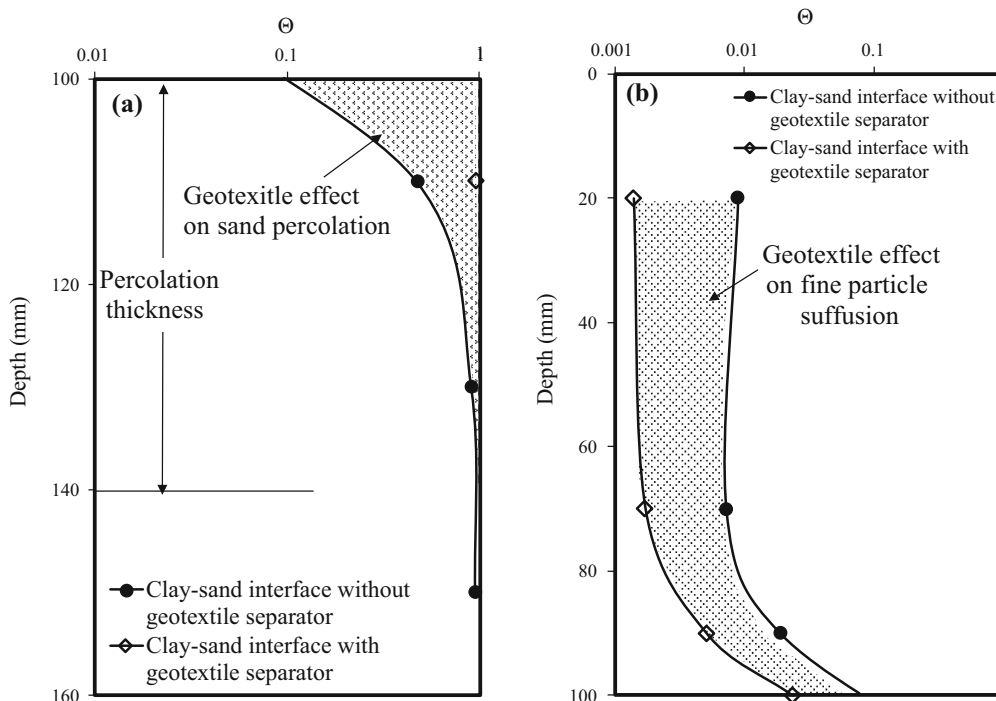


Fig. 13 Relative fine particle fraction along the soil profile for HKMD–sand interface region with and without a geotextile separator: **a** sand percolation and **b** fine particle suffusion

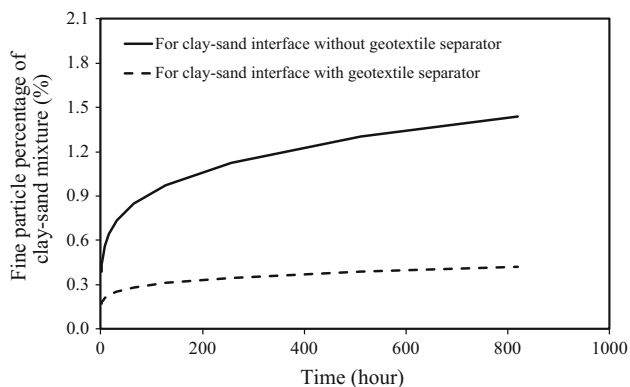


Fig. 14 Time versus fine particle percentage of clay–sand mixture at a depth of 100 mm due to suffusion at the clay–sand interface with and without a geotextile separator, predicted using Eq. (4)

$$\psi_{\text{fine},s}(t) = \int \frac{\gamma_w k_{er} \zeta i_w}{2\rho_{\text{clay}}} (1 - \phi_{\text{sand}} - \psi_{\text{fine}}) \left(\frac{\psi_{\text{fine},s}^0}{1 - \phi_{\text{sand}}} \right)^{2/3} \times \left\{ \left(\frac{\psi_{\text{fine},s}}{\psi_{\text{fine},s}^0} \right)^{2/3} - \left(\frac{i_c^0}{i_c^0 + i_w} \right) \right\} dt \tag{17}$$

As suggested by Bonelli and Marot [4], there is a function of fine particle immigration with the clay volume fraction

$$\Theta = \frac{(1 - \phi_{\text{micro}}) [\psi_{\text{fine},s}^0 - \psi_{\text{fine},s}(t)]}{(1 - \phi_{\text{micro}}) \psi_{\text{fine}}^0 + \phi_{\text{sand}}} \tag{18}$$

Combining Eq. (1) with Eq. (17), we can get

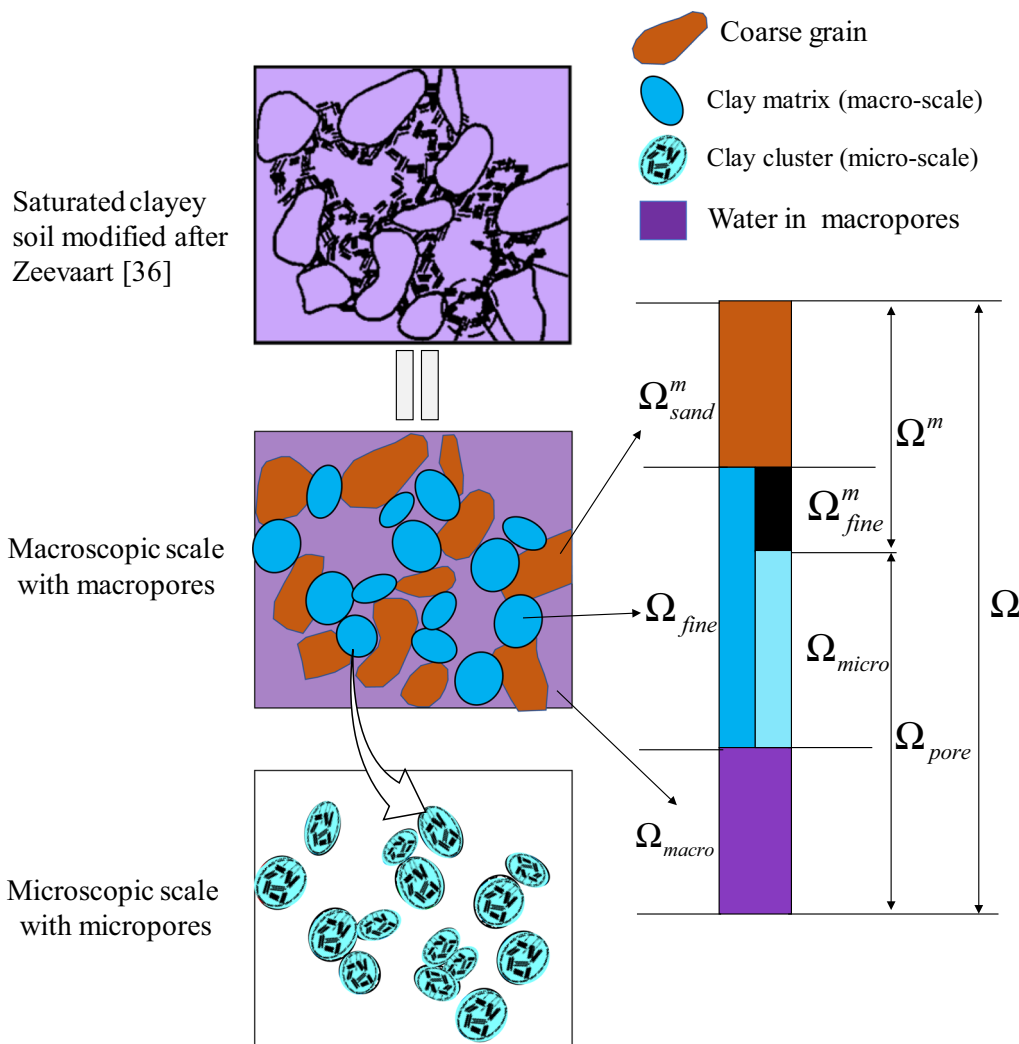


Fig. 15 Relative proportions of each constituent in the sand–clay sample

Table 2 Parameters values in the micromechanical modeling of the clay–sand interface without a geotextile separator

γ_w (N/m ³)	k_{er} (min/m)	ζ	i_w	ρ_{clay} (kg/m ³)
10,000	2×10^{-6}	1	20	2680
i_c^0	ψ_{fine}^0	ϕ_{sand}	ϕ_{micro}	δ
3	0.45	0.35	0.613	0.053

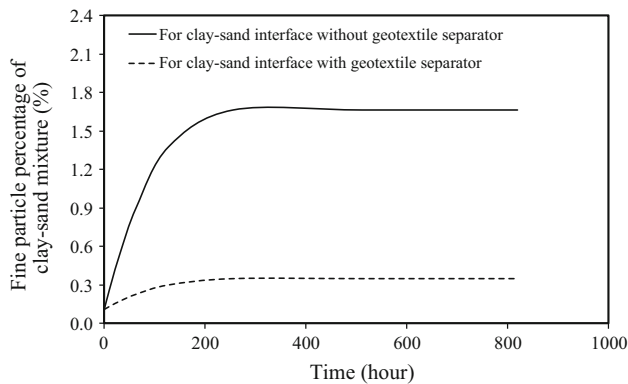


Fig. 16 Relationship of time versus fine particle percentage for the clay–sand mixture at a depth of 100 mm due to suffusion at the clay–sand interface with and without a geotextile separator, predicted using Eq. (19)

$$M_{mixture} = M_{clay} \left[\frac{(1 - \phi_{micro}) [\psi_{fine,s}^0 - \psi_{fine,s}(t)]}{(1 - \phi_{micro})\psi_{fine}^0 + \phi_{sand}} \right] + M_{sand} \tag{19}$$

The parameter values for the clay–sand interface without a geotextile separator are summarized in Table 2. The parameter determination is referred to Bonelli and Marot [4], and the value of δ is back-calculated from our test results (shown in Fig. 13b). The geotextile influences the values of k_{er} and δ because it mainly minimizes the surface erosion rate and migrated fine particle content. (The pore size of the geotextile will affect the migration of fine particles due to deposition or clogging.) For the clay–sand interface with a geotextile separator, $k_{er} = 1 \times 10^{-6}$ min/m and $\delta = 0.0089$. Using Eqs. (17) and (19), the fine particle percentage of the clay–sand mixture at the depth of 100 mm can be calculated and predicted, as shown in Fig. 16. The percentage of fine particle in the clay–sand mixture is stable after 300 h at 1.66%, which is very close to that measured in the test (1.77%). This is because the threshold hydraulic gradient is considered in the micromechanical modeling.

The fine particle suffusion and sand percolation observed in this physical model will likely occur in actual

reclamation and sedimentation projects when a geotextile separator is not utilized. The internal particle migration may lead to the failure of embankment dams and disks [2] and could lead to the loss of underlying soils in reclamation projects. Thus, it is necessary to account for the particle suffusion and sand percolation to exactly determine the amount of sand materials in the interface region. The findings in this study offer direct evidence for particle migration at the clay–sand interface when a geotextile separator is not used in the reclamation design. The micromechanical modeling and the empirical formula are adopted to interpret and analyze the particle suffusion during the consolidation stage, which helps to deepen understanding of this phenomenon and provide a tool to assess particle migration. However, in this physical model study, some limitations should be pointed out: factors such as mud waves, tidal effects, etc., which are usually generated in a reclamation project, were not considered in this experiment. These factors could perhaps induce a thicker sand percolation zone through the clay–sand interface if there is no geotextile separator. Furthermore, the spreading of sand fills in the physical model is uniform, which differs from the field practice and could affect the sand percolation and fine particle suffusion at the HKMD–sand interface. In other words, this study makes a special effort to investigate the influence of the geotextile separator on sand percolation and fine particle suffusion under specific conditions. More study is needed to further investigate and understand the effects of geotextile separators in situ.

4 Conclusions

In order to better understand the effects of a geotextile separator at the HKMD–sand interface in reclamation projects, a physical model was built, and an experimental test was performed by dividing the model into two parts: one part contained a clay–sand interface without a geotextile separator, while the clay–sand interface was incorporated with a geotextile separator in the other part. Particle migration was investigated during sand filling and the consolidation process of the HKMD layer. The PSD was compared before and after particle movement when no geotextile separator was used. The efficiency of the geotextile was illustrated by comparing the results at the clay–sand interface region with and without a geotextile separator, which gives some insight as to whether it is necessary to place a geotextile separator on the surface of HKMD in actual reclamation projects. Based on observations, test data and the analysis, the conclusions are as follows:

- (a) For the clay–sand interface without a geotextile separator, sand percolates into the clayey soil and the

fine particles from the clayey soils suffuse into the sand. Therefore, the actual clay–sand interface becomes an interfacial zone.

- (b) The analysis of the particle size distribution of soils retrieved from an excavated hole in the set apparatus reveal that the sand percolated to a depth of 40 mm and the fine particle suffusion decreased nonlinearly along the depth of clay–sand interface region when there was no geotextile separator at the interface between the HKMD and sand fill.
- (c) The geotextile separator prevented the sand particles from percolating into the clay surface. The geotextile separator effectively minimized the fine particle suffusion due to the bridge network. By comparing the behavior of the interface with and without a geotextile separator, it is proved that fine particle suffusion is an interfacial process rather than a volume process.
- (d) The maximum undrained shear strength of the soils in vicinity of the HKMD–sand interface was found to increase over time as consolidation progressed due to the change in the sand content at the clay–sand interface zone.
- (e) The relative fine particle fraction values along the depth were calculated using an empirical formula and a micromechanical model of the clay–sand interface with and without a geotextile separator, which is helpful to quantitatively analyze the effects of a geotextile separator for reclamation design.

Acknowledgements The work in this paper was financially supported by a consulting Project from China Harbour Engineering Company Limited (No. P16-0174), a National State Key Project “973” Grant (Grant No. 2014CB047000) (Sub-project No. 2014CB047001) from the Ministry of Science and Technology of the People’s Republic of China, a CRF Project (Grant No.: PolyU 12/CRF/13E) from the Research Grants Council (RGC) of Hong Kong Special Administrative Region Government (HKSARG) of China, two GRF Projects (PolyU 152196/14E; PolyU 152796/16E) from RGC of HKSARG of China. The authors also acknowledge the financial support from Research Institute for Sustainable Urban Development of The Hong Kong Polytechnic University, Grants (1-ZVCR, 1-ZVEH, 4-BCAU, 4-BCAW, 5-ZDAF, G-YN97). The authors wish to express special thanks to Dr. SHI X. S. for his kind help on this work.

References

1. Azadbakht S (2015) Analytical and experimental modeling of internal erosion in porous media. Doctoral dissertation, University of Alberta
2. Bonelli S (ed) (2012) Erosion of geomaterials. Wiley, Hoboken
3. Bonelli S, Marot D (2008) On the modelling of internal soil erosion, IACMAG. In: The 12th international conference of international association for computer methods and advances in geomechanics (IACMAG), Goa, India, pp 7–14
4. Bonelli S, Marot D (2011) Micromechanical modeling of internal erosion. *Eur J Environ Civ Eng* 15(8):1207–1224
5. Borja RI, Choo J (2016) Cam-Clay plasticity. Part VIII: a constitutive framework for porous materials with evolving internal structure. *Comput Methods Appl Mech Eng* 309:653–679
6. Borja RI, Koliji A (2009) On the effective stress in unsaturated porous continua with double porosity. *J Mech Phys Solids* 57(8):1182–1193
7. British Standards Institution (1990) Methods of test for soils for civil engineering purposes, BS 1377-2. BSI, London, pp 32–36
8. Choo J, White JA, Borja RI (2016) Hydromechanical modeling of unsaturated flow in double porosity media. *Int J Geomech* 16(6):D4016002
9. Choo H, Lee W, Lee C (2017) Compressibility and small strain stiffness of kaolin clay mixed with varying amounts of sand. *KSCE J Civ Eng* 21(6):2152–2161
10. Chu J, Varaksin S, Klotz U, Menge P (2009) Construction processes, state-of-the-art report (TC17, ISSMGE). In: Proceedings of the 17th international conference on soil mechanics and geotechnical engineering, Alexandria (Egypt)
11. Chung WB (2007) Filtration behavior and micro-observation of geotextiles under bi-directional cyclic flow. Master thesis, National Taiwan University (in Chinese)
12. Cividini A, Gioda G (2004) Finite-element approach to the erosion and transport of fine particles in granular soils. *Int J Geomech* 4(3):191–198
13. Cividini A, Bonomi S, Vignati GC, Gioda G (2009) Seepage-induced erosion in granular soil and consequent settlements. *Int J Geomech* 9(4):187–194
14. Fell R, Fry JJ (2007) Internal erosion of dams and their foundations. In: Selected and reviewed papers from the workshop on internal erosion and piping of dams and their foundations, Aussois, France, 25–27 April 2005. Taylor & Francis Group
15. Feng WQ, Lalit B, Yin ZY, Yin JH (2017) Long-term non-linear creep and swelling behavior of Hong Kong marine deposits in oedometer condition. *Comput Geotech* 84:1–15
16. Foot R, Koutsoftas DC, Handfelt LD (1987) Test fill at Chek Lap Kok, Hong Kong. *J Geotech Eng* 113(2):106–126
17. Fukue M, Okusa S, Nakamura T (1986) Consolidation of sand-clay mixtures. In: Yong RN, Townsend FC (eds) Consolidation of soils: testing and evaluation, ASTM STP892. American Society for Testing and Materials, Philadelphia, pp 627–641
18. Furudoi T, Kobayashi M (2007) A case history of Kansai International Airport phase II projects, large-scale reclamation works on soft deposits. *ISSMGE Bull* 1(4):3–6
19. Golay F, Bonelli S (2011) Numerical modeling of suffusion as an interfacial erosion process. *Eur J Environ Civ Eng* 15(8):1225–1241
20. Gutiérrez F, Guerrero J, Lucha P (2008) A genetic classification of sinkholes illustrated from evaporite paleokarst exposures in Spain. *Environ Geol* 53(5):993–1006
21. Ho CC (2007) The erosion behaviour of revetment using geotextile. PhD thesis, Joseph Fourier University, Grenoble, France
22. Kenney TC, Lau D (1985) Internal stability of granular filters. *Can Geotech J* 22(2):215–225
23. Kenny TC (1977) Residual strength of mineral mixtures. In: Proceedings of the 9th international conference on soil mechanics, vol 1. Japanese Geotechnical Society, Tokyo, pp 155–160
24. Mackay AD, Wightman NR (2016) Design and construction considerations for reclamations and the use of vibro-flotation to accelerate settlement. *HKIE Geotech Div Annu Semin* 2016:73–88
25. Monkul MM, Ozden G (2007) Compressional behavior of clayey sand and transition fines content. *Eng Geol* 89(3):195–205

26. Park J, Santamarina JC (2017) Revised soil classification system for coarse–fine mixtures. *J Geotech Geoenviron Eng* 143(8):04017039
27. Peters JF, Berney ES IV (2009) Percolation threshold of sand–clay binary mixtures. *J Geotech Geoenviron Eng* 136(2):310–318
28. Shi XS, Herle I (2016) Analysis of the compression behavior of artificial lumpy composite materials. *Int J Numer Anal Methods Geomech* 40(10):1438–1453
29. Shi XS, Herle I (2017) Numerical simulation of lumpy soils using a hypoplastic model. *Acta Geotech* 12(2):349–363
30. Shi XS, Herle I (2017) A model for natural lumpy composite soils and its verification. *Int J Solids Struct* 121:240–256
31. Shi XS, Yin J (2017) Consolidation behavior for saturated sand–marine clay mixtures considering the intergranular structure evolution. *J Eng Mech* 144(2):04017166
32. Shi XS, Yin JH (2017) Experimental and theoretical investigation on remolded sand–marine clay mixtures within homogenization framework. *Comput Geotech* 90:14–26
33. Sibille L, Marot D, Sail Y (2015) A description of internal erosion by suffusion and induced settlements on cohesionless granular matter. *Acta Geotech* 10(6):735–748
34. Simpson DC, Evans TM (2015) Behavioral thresholds in mixtures of sand and kaolinite clay. *J Geotech Geoenviron Eng* 142(2):04015073
35. Skempton AW (1964) Long-term stability of clay slopes. *Géotechnique* 14(2):77–102
36. Sterpi D (2003) Effects of the erosion and transport of fine particles due to seepage flow. *Int J Geomech* 3(1):111–122
37. Van't Hoff J, Van der Kolff AN (eds) (2012) *Hydraulic fill manual: for dredging and reclamation works*, vol 244. CRC Press, Leiden
38. Yin J-H (1999) Properties and behaviour of Hong Kong marine deposits with different clay contents. *Can Geotech J* 36(6):1085–1095
39. Yin JH, Fang Z (2010) Physical modeling of a footing on soft soil ground with deep cement mixed soil columns under vertical loading. *Mar Georesour Geotechnol* 28(2):173–188
40. Yin ZY, Hattab M, Hicher PY (2011) Multiscale modeling of a sensitive marine clay. *Int J Numer Anal Methods Geomech* 35(15):1682–1702
41. Yin ZY, Zhao J, Hicher PY (2014) A micromechanics-based model for sand–silt mixtures. *Int J Solids Struct* 51(6):1350–1363
42. Zeevaart L (1986) Consolidation in the intergranular viscosity of highly compressible soils. In: ASTM (ed) *Consolidation of soils: testing and evaluation*, vol 892. ASTM Special Technical Publication, Philadelphia, pp 257–281

Publisher's Note Springer Nature remains neutral with regard to jurisdictional claims in published maps and institutional affiliations.